Locking Bandwidth and Relaxation Oscillations of an Injection-Locked Semiconductor Laser

ISABELLE PETITBON, PHILIPPE GALLION, MEMBER, IEEE, GUY DEBARGE, AND CLAUDE CHABRAN

Abstract—**A theoretical and experimental study of an injection-locked semiconductor laser is reported. Typical results concerning the position and the size of the locking bandwidth are given and compare favorably to the calculated ones, thus validating the developed modelization of the injected laser. The effect of synchronization on the intensity level is pointed out. Then the interest of the technique in terms of modulation is estimated by investigating the behavior, amplitude, and frequency of the relaxation oscillations which are the main limiting factor in this case.**

I. Introduction

SEMICONDUCTOR lasers exhibit several intrinsic characteristics such as partition noise, mode instability, and broad linewidth, which are prejudicial to their use in coherent optical communication systems. As injection locking had already proven successful for different kinds of oscillators [1]–[3], its application for semiconductor lasers aroused great interest. It was indeed likely to improve coherence properties of the emitted signal and to give rise to various applications. Numerous studies conducted on the subject have shown encouraging prospects: suppression of mode hopping, lowering of the partition noise [4], reduction of the relaxation oscillations under direct modulation [5], [6], and linewidth narrowing [7]. In addition to the above-mentioned improvements, injection locking offers several advantages in view of coherent telecommunications such as the possibility of frequency to phase modulation conversion, and the achievement of locked local oscillators. In the development of semiconductor laser arrays, injection locking has been demonstrated to operate conveniently by synchronizing an array of lasers onto a unique master [8].

Injection locking may also prevent spurious feedback effects which are difficult to avoid and can strongly disturb the behavior of the laser. As this feedback is very sensitive to external influences, in particular to mechanical vibrations and temperature, and as its effects are somewhat random, a stable injection locking may overcome them, provided that the injection level is high enough.

Furthermore, injection locking is a method of investigating laser properties, the injected beam acting as a probe inside the slave cavity. The resulting signal provides information on the gain curve [9], the carrier number change due to injected photons, and the consequent variation of the refractive index [10], or the damping of relaxation oscillations [11]. Furthermore, the position and the width of the locked region are strongly dependent on the phase–amplitude coupling, which is a phenomenon specific to semiconductor lasers [12]–[14].

However, the above conclusions concerning the locked laser behavior have to be made more precise, for they strongly depend on parameters such as the injection rate and the position of the injected frequency in the gain curve of the laser. Thus, the conditions of operation have to be taken carefully into account in order to evaluate the applicability of the method to optical communications.

The work presented in this paper is aimed at describing the effects of injection locking on the output signal spectrum, as a function of the injection rate and the frequency detuning between the master and free-running laser fields, and at discriminating their advantages and drawbacks, in view of communication applications. In Section II, we consider the achievement of optical synchronization. We derive theoretical results for the locking bandwidth and report original experimental measurements of the position and width of the locking range. The free-running and locked output powers are measured for different operating points and the power change through the locking bandwidth is compared to experimental results. Next, in Section III, we focus on the dramatic evolution of the power spectrum when the operating point is moved through the locked area: injection modifies the damping mechanism of the relaxation oscillations, giving rise to exaggerated lateral peaks in the intensity spectrum and decreasing considerably the laser coherence. This weak damping of the relaxation oscillations will be a major limiting factor in the modulation of the locked laser. Finally, we discuss necessary conditions for obtaining an efficient injection locking.

II. Locking Mechanism

We consider two semiconductor lasers chosen so that they both are monomode and emit in the same wavelength range. The light of one laser, referred to as the master laser (ML), is injected into the second one, called the slave laser (SL). An optical isolator prevents reciprocal coupling.

By carefully adjusting the currents and temperatures of the lasers, the slave cavity is made resonant, or near so,

Manuscript received May 16, 1987; revised September 11, 1987.

The authors are with the Ecole Nationale Supérieure des Télécommunications, 75634 Paris Cedex 13, France.

IEEE Log Number 8718258.

with the master optical field, which is then amplified since there is gain available. Depending on the injection level and the laser frequencies, the master field saturates the gain more or less strongly [9]. Therefore, it is not necessary that the two frequencies be very close together to achieve synchronization, but then the locking may not be complete; this means that, of itself, the injection level is not high enough to saturate the gain and to extinguish all the free-running modes. In that case, our experimental setup leads to bimodal behavior, and the energy is distributed between the free-running and locked modes, the latter being at the master frequency. However, the operating conditions most often permit complete locking. We will limit the analysis in the following development to this case, for it is the most interesting and efficient, as well as the simplest theoretically.

A. Theory

Under the previous conditions, the usual plane-wave and slowly varying envelope approximation of the electric field inside the injected cavity leads to the well-known rate equations for the total photon number P and the phase ϕ [15].

$$\dot{P} = \left[G - 1/\tau_P + \frac{c}{n_g L}\left(\frac{P_i}{P}\right)^{1/2} \cos\theta \right] P \qquad (1)$$

$$\dot{\phi} = \left[\omega_{mo} - \omega_o + \frac{c}{2n_g L}\left(\frac{P_i}{P}\right)^{1/2} \cdot \sin\theta + \frac{\alpha}{2}(G - 1/\tau_p) \right]. \qquad (2)$$

G is the optical gain approximated by $\Gamma A(N - N_o)$ where Γ is the confinement factor, A is the differential gain, N is the carrier number, and N_o is the carrier number for transparency. τ_p is the photon lifetime, L the cavity length, n_g the group index, and c the light velocity. α accounts for the phase–amplitude coupling in the electric field [12]. P_i represents the number of injected photons in the cavity and θ the phase difference $\phi_i - \phi$ between the injected and the free-running fields. ω_o is the angular frequency of the master laser and ω_{mo} is the unperturbed cavity frequency which is the closest to ω_o and the frequency detuning between the two laser fields $\omega_o - \omega_{mo}$ will be noted $\Delta\omega$.

The equations have been suitably normalized so that P equals the square amplitude $|E|^2$ of the electric field.

A third equation for the carrier number completes the description of the system:

$$\dot{N} = \frac{I}{e} - GP - \frac{N}{\tau_e} \qquad (3)$$

where I is the injection current, e the electronic charge and τ_e the spontaneous electron lifetime. Fluctuation driving terms are neglected at first.

B. Locking Bandwidth

The search of the steady-state solutions of the system, $\bar{P}$, $\bar{N}$, $\bar{\theta}$, characterizes the laser operating point and constitutes the first step in the study of the locking bandwidth.

From (1) and (2), the expression of the locking bandwidth is given as a function of the injection rate $(c/2n_gL) \cdot (P_i/P)^{1/2}$ and the phase difference θ:

$$\Delta\omega = \frac{c}{2n_gL}\left(\frac{P_i}{P}\right)^{1/2} \cdot (\sin\theta - \alpha\cos\theta). \qquad (4)$$

$\Delta\omega$ appears there as a sum of two contributions [13]. The first represents the detuning $\omega_o - \omega_{mi}$ between the master and injected slave cavity angular frequencies; it is the usual frequency shift, appearing in every locking mechanism, and was first introduced by Adler [1]. The second part of expression (4) accounts for the cavity frequency shift due to optical injection $\omega_{mi} - \omega_{mo}$. It is an extra term peculiar to semiconductor lasers, arising from the refractive index dependence on carrier density.

By setting $\rho = (c/2n_gL) \cdot (P_i/P)^{1/2}$ and $\theta_0 = \tan^{-1}(\alpha)$, we rewrite $\Delta\omega$ as $\rho\sqrt{1+\alpha^2} \cdot \sin(\theta - \theta_0)$. The sine law, due to the Adler's phase difference, sets a first limitation on the locking bandwidth and consequently $|\Delta\omega|$ remains less than $\rho\sqrt{1+\alpha^2}$.

Another physical restriction comes from the ability of the laser to oscillate at the master frequency. The forced oscillation competes with the amplification of the spontaneous emission and prevails over it if the net gain of the medium in the locked state $(G - 1/\tau_p)$ is negative [16]. This condition implies an important reduction to the acceptable θ excursion: between $-\pi/2$ and $\pi/2$ only. Consequently $\Delta\omega$ is bounded by

$$-\rho\sqrt{1+\alpha^2} < \Delta\omega < \rho. \qquad (5)$$

The locking bandwidth clearly appears asymmetric because of the phase–amplitude coupling.

As the locked-slave laser oscillates at a unique frequency, it is convenient to introduce a more intuitive approach of the phenomenon. The optical field is represented on a phasor diagram, as the sum of the free-running $(\sqrt{P_f}, \phi)$ and injected $(\sqrt{P_i}, \phi_i)$ contributions; the axes of the diagram are the real and imaginary parts of the electric field (Fig. 1). From the condition $-\pi/2 < \theta < \pi/2$, the locked laser operating points fall above the dashed line, and it is clear that injection locking is a constructive interaction with regard to the power balance since the total locked power is always greater than the free-running one.

The detailed study of the detuning $\Delta\omega$ as a function of the phase difference shows that the variations are not monotonic; at every detuning between $-\rho\sqrt{1+\alpha^2}$ and $-\rho$ correspond two possible values of θ, with two gain levels [16]. The long-term stable state is the one requiring the weaker gain at threshold. The θ range $[-\pi/2, -\pi/2 + \tan^{-1}\alpha]$ is then excluded for a long-term synchronization, but it may be reached if hysteresis occurs and provides an opportunity for bistability.

Yet the problem of stability has not been completely addressed. The laser is stable if it comes back to its operating point after undergoing slight perturbations dP, dN,

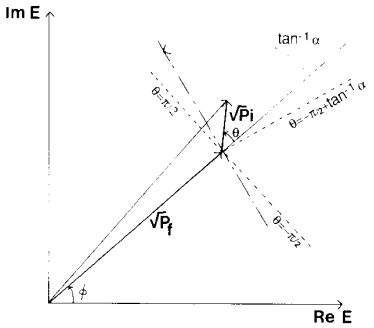

Fig. 1. Phasor diagram sketching the injection locking effect. The dashed lines (- - - -) mark the maximum excursion of θ and the other dashed line (—— - - ——) is the loci of relaxation oscillations introduced in Section III.

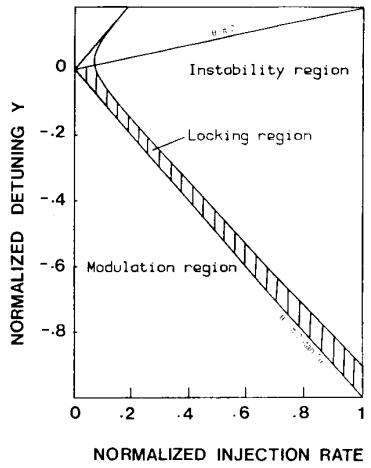

Fig. 2. Synchronization region (hatched area) and other operating regions under optical injection as a function of the injection rate and the detuning between the two fields. The boundary specified by $\theta = -\pi/2 + \tan^{-1}\alpha$ corresponds both to the highest frequency of the locking range and the maximum detuning (taken as an absolute value).

$d\theta$. To verify this condition, we first linearize the rate equations in the form

$$\begin{bmatrix} d\dot{P}/\omega_{RO}^2\tau_p \\ d\dot{N} \\ 2Pd\dot{\theta}/\omega_{RO}^2\tau_p \end{bmatrix} = \begin{bmatrix} -\rho\cos\theta & 1 & -\rho\sin\theta \\ \omega_{RO}^2(2\rho\tau_p\cos\theta - 1) & -2/\tau_R & 0 \\ \rho\sin\theta & -\theta & -\rho\cos\theta \end{bmatrix} \cdot \begin{bmatrix} dP/\omega_{RO}^2\tau_p \\ dN \\ 2Pd\theta/\omega_{RO}^2\tau_p \end{bmatrix} \quad (6)$$

with the additional notation $\tau_R = 2(1/\tau_e + \Gamma AP)^{-1}$ and $\omega_{RO}^2 = (\Gamma AP/\tau_p)^{1/2}$.

Finally we use the Routh–Hurwitz criteria which apply to any linearized system and constitute a set of necessary conditions for stable behavior. They are

$$\text{tr}\,(M) \geq 0 \quad (7a)$$

$$\det(M) \geq 0 \quad (7b)$$

$$\det(M) \leq \text{tr}\,(M) \cdot \sum_i m_{ii} \quad (7c)$$

where M is the above 3×3 matrix describing the system evolution, tr (M) its trace, det (M) its determinant, and the m_{ii} its minors.

The first condition is automatically satisfied if the inequality (5) is fulfilled. The two others lead to complicated and tedious calculations if completely developed. However, usual experimental conditions allow us to make some approximations:

$$\rho\tau_p \ll 1 \qquad \rho/\tau_R \ll \omega_{RO}^2 \quad \text{and} \quad \rho \ll \omega_{RO}.$$

Therefore, under the assumption of a weak injection rate, $P_i/P < 10^{-3}$, the system reduces to

$$2/\tau_R > \rho(\alpha\sin\theta - \cos\theta) = \rho\sqrt{1+\alpha^2}\cos\left[\pi - (\theta + \tan^{-1}\alpha)\right]. \quad (8)$$

From (8) it is seen that for a sufficiently low injection rate, $\rho < 2/(\tau_R\sqrt{1+\alpha^2})$, the laser remains unconditionally stable.

For higher injection rates, inequality (8) defines the low frequency limit of the synchronization and the minimum absolute value of detuning. It corresponds to an arc of hyperbola, the equation of which is derived from (8). The locking bandwidth is there limited to a narrow range of θ values.

Fig. 2 illustrates these conclusions and displays the synchronization area (hatched area) on a graph showing the normalized detuning $y = (\Delta\omega\tau_R)/(1+\alpha^2)$ as a function of the normalized injection rate $x = (\rho\ \tau_R)/\sqrt{1+\alpha^2}$. The other regions of operation shown are introduced in the following.

Before going on, it is worth noting that the allowed detuning is negative for injection rates higher than $\rho = 2/\sqrt{1+\alpha^2}$ and it is more convenient to consider its absolute value in the following. In that case, the high-frequency limit of synchronization corresponds to the maximum detuning and the low-frequency limit corresponds to the minimum detuning.

C. Experimental Results

In parallel, experiments were carried out investigating the laser behavior for various injection rates.

Two CSP-AlGaAs lasers (Hitachi 1400) were used, both of which were thermally stabilized within a few hundredths of a degree by thermoelectric elements. Numerical values of the device parameters are $L = 300\ \mu\text{m}$, $n_g = 4.3$, $\alpha = 5$.

Fig. 3 represents the experimental setup. The output beam is passed through a spectrometer and then through a Fabry–Perot interferometer. The spectrometer allows a precise determination of the different mode wavelengths, serves as a filter of spontaneous emission, and eliminates

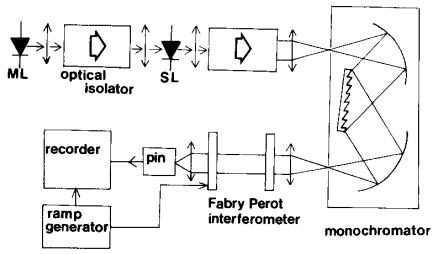

Fig. 3. Experimental setup.

residual mode effects in the Fabry–Perot. The free-running and locked output powers are recorded from the monitor beam.

Before the locking occurs, on the high-frequency side of the locked area, that is with the maximum detuning, the optical injection induces a modulation in the free-running signal [17] while the output power remains constant. When the detuning reaches $\Delta\omega_{max}$, the free-running mode disappears and the oscillation locks onto the master frequency; simultaneously the power increases rapidly and reaches its maximum at a very near point. Then, as the detuning keeps decreasing, the power gain is reduced but does not vanish completely, for the evolution is stopped by stability considerations. At the low-frequency boundary, the locked laser becomes unstable [18]. The laser becomes multimode and the damping of the relaxation oscillations vanishes. The loss of synchronization is therefore difficult to determine precisely: although the dominant lasing mode remains at the injected frequency, spurious free-running modes increase gradually.

Fig. 4 displays an enlargement of a part of Fig. 2, in which operating points are plotted. These are determined by calculating x and y from P_i, P, and $\Delta\omega$ measurements. $\Delta\omega_{max}$ is obtained either by measuring ω_o and ω_{mo} separately or by directly reading the difference $\Delta\omega$, at the limit of synchronization, when it is less than the free-spectral range of the Fabry–Perot; then the operating point is moved through the locking bandwidth by increasing the slave current, thus decreasing slightly the injection rate. The equivalent free-running frequency is assumed to vary at the ordinary rate -3 GHz/mA, allowing a calculation of $\Delta\omega$ for every point. The width of the locking range reaches up to 10 GHz when P_i/P is about 10^{-3}, that is the maximum valid level of our approximations. The average locking bandwidth in Fig. 4 is 4–6 GHz.

D. Locked Power

As previously mentioned, injection locking affects the output power of the slave laser [16]. Under the assumption of a weak injection, $P_i/P < 10^{-3}$, Fig. 1 allows us to write the total photon number as

$$P = P_f + 2\sqrt{P_f P_i} \cdot \cos\theta.$$

In terms of optical power P_u, the equality becomes

$$P_u = P_{uf} + \left(2\frac{\tau_p}{\tau_m} \cdot P_{uf}P_{ui}\right)^{1/2} \cdot \cos\theta$$

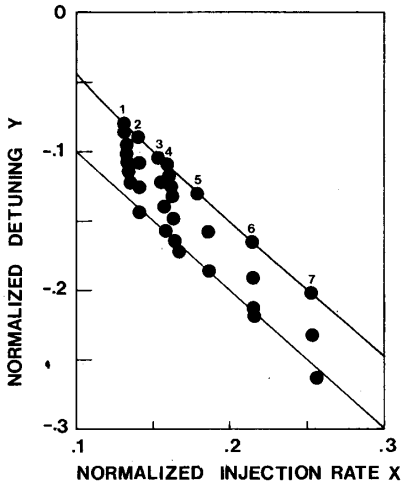

Fig. 4. Theoretical locking bandwidth (solid lines) and series of experimental locked points through the locking bandwidth.

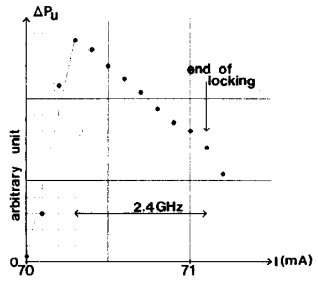

Fig. 5. Output power variations through the locking bandwidth as a function of the injection current. The abrupt side corresponds to the maximum absolute value of the detuning, on the high-frequency boundary of the locking bandwidth.

with τ_m being the decay time associated with the facet losses only.

Finally synchronization produces an output power change ΔP_u:

$$\Delta P_u = \left(2\frac{\tau_p}{\tau_m} \cdot P_{uf}P_{ui}\right)^{1/2} \cdot \cos\theta$$

$$\Delta P_u = \frac{1}{\alpha}\left(2\frac{\tau_p}{\tau_m} \cdot P_{uf}P_{ui}\right)^{1/2} \cdot \left(\sin\theta - \frac{\Delta\omega}{\rho}\right).$$

For our experimental points, the rate $\Delta\omega/\rho$ is largely greater than $\sin\theta$ and a linear dependence of ΔP_u on $\Delta\omega$ is observed. Fig. 5 gives an example of the output power change through the locking bandwidth.

III. Relaxation Oscillations

As previously noted, no attention was paid in the above analysis to quantum fluctuations that continuously occur and disturb the laser emission. This simplification was justified as long as the study was focused on stability and locking mechanisms. However, noise has to be included in order to gain further knowledge of the laser line characteristics; the noise is a combination of the noise of the

slave oscillator itself and the fluctuations of the injected signal. One way to take this into account is to complete the rate equations (1)–(3) with usual Langevin force terms [19], [20]. An extensive simulation of noise in injection-locked semiconductor lasers has been achieved by Schunk and Petermann [14].

The equations are then linearized and, after a Fourier transform, the noisy locked laser is described by a linear system parameterized by the angular frequency ω.

At this stage, two levels of approximation may be adopted depending on the result sought. The simpler one takes into account the spontaneous emission coupled in the lasing mode, but it neglects the dynamics of the gain saturation. Such an approach leads to calculations of the laser linewidth and of the intensity noise spectrum. This has been developed extensively in numerous works for free-running lasers [19]–[22]. In this paper, study is focused on describing and explaining the fine structure of the intensity spectrum of the locked laser, and its evolution through the locking bandwidth. The gain saturation plays a key role since its relaxation mechanisms give rise to lateral peaks or sidebands in the intensity spectrum [23]. These are observed through a Fabry–Perot interferometer with a 10 GHz free spectral range. They have been observed in various types of semiconductor lasers, and their intensities are on the order of 1 per cent of the main peak, or even less [21]–[24]. Fig. 6 displays a typical spectrum of the free-running slave laser; it exhibits lateral peaks slightly higher than expected. This is most probably due to some undesired feedback.

Nonetheless, the gain saturation dynamics are strongly disturbed under optical injection, and even more so under synchronization, as will be demonstrated below.

Considering again the above mentioned Fourier transform matrix, we obtain a third degree equation in $j\omega$, the solutions of which provide the parameters of the transient regime in the form

$$\omega_1 = j/\tau_R'' \tag{9a}$$

$$\omega_2 = \omega_R' + j/\tau_R' \tag{9b}$$

$$\omega_3 = -\omega_R' + j/\tau_R'. \tag{9c}$$

The last two solutions, which contain both an imaginary and a real term, express the modified relaxation oscillation frequency ω_R' and damping time τ_R' of the injected laser and contain information concerning the modification of the sidebands in the locked laser.

When ρ is small compared to $1/\tau_p$, we may expand the angular frequency ω_R' and the associated damping time τ_R' as functions of the free-running parameters ω_{RO} and τ_R as follows

$$\omega_R'^2 = \omega_{RO}^2 - 1/\tau_R'^2 \tag{10a}$$

$$2/\tau_R' = 2/\tau_R + \rho(\cos\theta - \alpha \sin\theta). \tag{10b}$$

The most dramatic effect is the action of injection locking on the damping time since it depends on the sign of $(\cos\theta - \rho \sin\theta)$ and is a rapidly varying function of θ; the greater the value of ρ, the more pronounced is this effect.

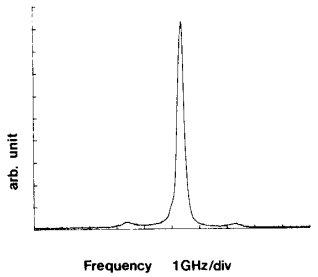

Fig. 6. Free-running intensity spectrum of the slave laser.

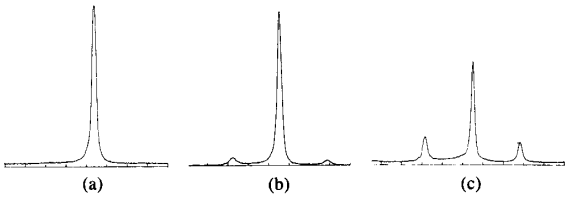

Fig. 7. Evolution, through the locking bandwidth, of the intensity spectrum, showing up lateral peaks arising from relaxation oscillations. The three spectra refer to the series numbered 7 on Fig. 4 and are arranged in order of decreasing $|\Delta\omega|$. The abscissa is graduated in gigahertz.

It is of great interest to increase the damping in order to obtain a signal as Lorentzian as possible, that is, the finest physical line [7]. The condition $1/\tau_R' > 1/\tau_R$, which is needed to obtain this result, is fulfilled for the large detunings of the locking bandwidth. This region is limited by the reduced detunings $-\rho\sqrt{1+\alpha^2}$ and $-\rho(1-\alpha^2)/\sqrt{1+\alpha^2}$, corresponding to values of θ between $-\pi/2 + \tan^{-2}\alpha$ and $\pi/2 - \tan^{-1}\alpha$, respectively.

Once again we now deal with the absolute value of the detuning. At the maximum detuning boundary, τ_R' reaches a minimum $[1/\tau_R - \rho(\alpha/\sqrt{1+\alpha^2})]$ [Fig. 7(a)]. With decreasing detuning, τ_R' increases continuously and equals the free-running damping time for $\theta = \pi/2 - \tan^{-1}\alpha$. Beyond this limit, synchronization is no longer favorable to sideband reduction. The lateral peak amplitude increases rapidly [Fig. 7(b) and (c)]. At the minimum detuning boundary, $1/\tau_R' = 0$, the relaxation oscillations are no longer damped and the laser undergoes instabilities, leading to the loss of synchronization [18], except when a low value for ρ prevents $1/\tau_R'$ from becoming zero. The necessary condition $\rho < 2/(\tau_R\sqrt{1+\alpha^2})$ has been previously encountered for the static stability of the system.

These results may also be displayed on the phasor diagram introduced in the preceding section. The influence of injection locking on relaxation oscillations is visualized in Fig. 1 by projecting the injected vector $(\sqrt{P_i}, \phi_i)$ on the loci of relaxation oscillations which is represented by the dashed line making an angle θ with the free-running vector $(\sqrt{P_f}, \phi)$. The extent of the damping time depends on the size of the projection, and it is clear that $\tau_R' = \tau_R$ when the injected field is orthogonal to this dashed

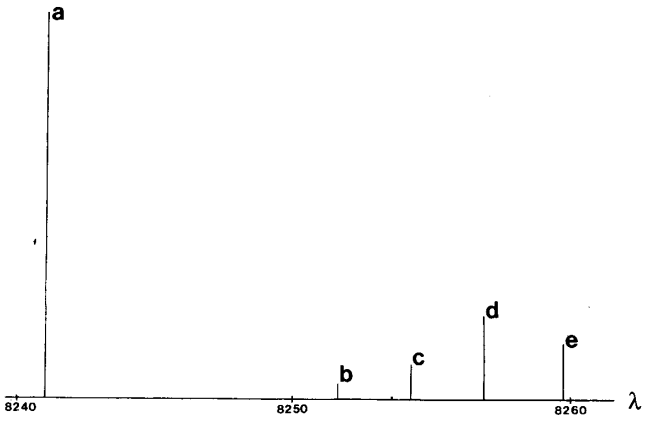

Fig. 8. Excited modes in the slave cavity when the damping of the relaxation oscillations decreases over the free-running level: the locked mode at 8241 Å (a), and cavity modes at 8251.6 Å (b), 8254.2 Å (c), 8256.9 Å (d), and 8259.7 Å (e), respectively; the free-running wavelength is 8256.9 Å.

line, i.e., for the previously derived value of $\theta = \pi/2 - \tan^{-1} \alpha$. At this point, relaxation oscillations are not influenced by the optical injection.

Furthermore, experimental observations have shown that the increase of the relaxation oscillations sidebands coincides with the degradation of the single-frequency operation; free-running spurious modes which are attenuated for the largest detunings increase again. However, the laser is locked, the main lasing mode being at the master frequency. When the operating point is shifted toward the minimum detuning limit, the spectrum exhibits the locked mode and several spurious modes of the free-running cavity (Fig. 8). As the damping time of these oscillations increases, the laser becomes more and more multimode. Each mode of Fig. 8 exhibits a fine structure resolved through the Fabry–Perot interferometer as displayed on Fig. 9 [25].

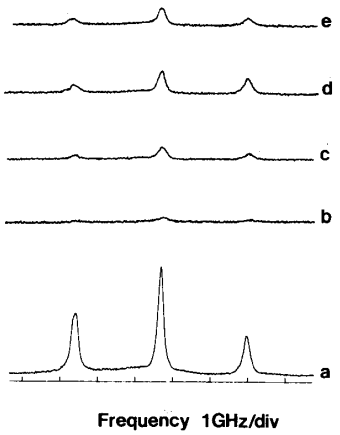

Fig. 9. Intensity spectra of the modes displayed in Fig. 8. The ordinate unit is arbitrary but the same for the five spectra.

Conclusion

A detailed study of the locking bandwidth and the relaxation oscillations of an injection-locked semiconductor laser has been presented. Measurements of the locking bandwidth as a function of the injection rate were found to be in good agreement with theoretical predictions, which allowed validation of the model elaborated to describe the system. The output power change has also been investigated and was found to vary linearly with the detuning when θ is small. In addition, the fine structure of the intensity spectrum revealed a dramatic evolution of the damping of the relaxation oscillations when the detuning and the phase difference between the two fields vary through the locking bandwidth. The damping of these oscillations is of great interest in order to evaluate the potential modulation performance of such a laser.

Injection locking can offer a locking bandwidth up to about 10 GHz with a ratio P_i/P in the range 10^{-3}–10^{-4}. However, θ variations are then limited to a rather narrow range less than $\pi/4$. Moreover, a part of this area seems to be difficult to use for coherent optical communications since the intensity spectrum exhibits high lateral peaks due to relaxation oscillations.

The influence of these phenomena is expected to weaken considerably and even to disappear as the injection rate decreases and becomes less than the threshold of unconditional stability. In parallel, θ is authorized to vary over a larger interval, which improves the conditions for performing a frequency to phase modulation conversion, and the sideband frequency no longer limits the modulation frequency.

References

[1] R. Adler, "A study of locking phenomena in oscillators," *Proc. IRE*, vol. 34, pp. 351–357, June 1946.
[2] H. L. Stover and W. H. Steier, "Locking of laser oscillators by light injection," *Appl. Phys. Lett.*, vol. 8, pp. 91–93, Jan. 1966.
[3] K. Kurokawa, "Injection-locking of microwave solid-state oscillators," *Proc. IEEE*, vol. 61, pp. 1386–1408, Oct. 1973.
[4] K. Iwashita and K. Nakagawa, "Suppression of mode partition by

laser diode light injection," *IEEE J. Quantum Electron.*, vol. QE-18, pp. 1669-1674, Oct. 1982.
[5] R. Lang, "Injection locking properties of a semiconductor laser," *IEEE J. Quantum Electron.*, vol. QE-18, pp. 976-983, June 1982.
[6] F. Mogensen, H. Olesen, and G. Jacobsen, "FM noise suppression and linewidth reduction in an injection-locked semiconductor laser," *Electron. Lett.*, vol. 21, pp. 696-697, Aug. 1985.
[7] P. Gallion, H. Nakajima, G. Debarge, and C. Chabran, "Contribution of spontaneous emission to the linewidth of an injection-locked semiconductor laser," *Electron. Lett.*, vol. 21, pp. 626-628, July 1985.
[8] L. Goldberg, H. L. Taylor, J. F. Weller, and D. R. Scifres, "Injection locking of coupled-strip diode laser arrays," *Appl. Phys. Lett.*, vol. 46, pp. 236-238, Mar. 1985.
[9] L. Goldberg, H. F. Taylor, and J. F. Weller, "Intermodal injection locking and gain profile measurement of GaAlAs lasers," *IEEE J. Quantum Electron.*, vol. QE-20, pp. 1226-1229, Nov. 1984.
[10] D. M. Fye, "Relationship between carrier-induced index change and feedback noise in diode lasers," *IEEE J. Quantum Electron.*, vol. QE-18, pp. 1675-1678, Oct. 1982.
[11] I. Petitbon, P. Gallion, G. Debarge, and C. Chabran, "Locking bandwidth and relaxation oscillations of an injection locked semiconductor laser," *Electron. Lett.*, vol. 22, pp. 889-890, Aug. 1986.
[12] C. H. Henry, "Theory of the linewidth of semiconductor lasers," *IEEE J. Quantum Electron.*, vol. QE-18, pp. 259-264, Feb. 1982.
[13] P. Gallion and G. Debarge, "Influence of amplitude-phase coupling on the injection locking bandwidth of a semiconductor laser," *Electron. Lett.*, vol. 21, pp. 264-266, Mar. 1985.
[14] N. Schunk and K. Petermann, "Noise analysis of injection-locked semiconductor injection lasers," *IEEE J. Quantum Electron.*, vol. QE-22, pp. 642-650, May 1986.
[15] G. P. Agrawal, "Generalized rate equations and modulation characteristics of external cavity semiconductor laser," *J. Appl. Phys.*, vol. 56, pp. 3110-3115, Dec. 1984.
[16] C. H. Henry, N. A. Olsson, and N. K. Dutta, "Locking range and stability of injection locked 1.54 μm InGaAsP semiconductor lasers," *IEEE J. Quantum Electron.*, vol. QE-21, pp. 1152-1156, Aug. 1985.
[17] P. Gallion, G. Debarge, and C. Chabran, "Output spectrum of an unlocked optically driven semiconductor laser," *Opt. Lett.*, vol. 11, pp. 67-69, May 1986.
[18] F. Mogensen, H. Olesen, and G. Jacobsen, "Locking conditions and stability properties for a semiconductor laser with external light injection," *IEEE J. Quantum Electron.*, vol. QE-21, pp. 784-793, July 1985.
[19] P. Spano, S. Piazzolla, and M. Tamburrini, "Phase noise in semiconductor lasers; A theoretical approach," *IEEE J. Quantum Electron.*, vol. QE-19, pp. 1195-1199, July 1983.
[20] C. Henry, "Theory of the phase noise and power spectrum of a single mode injection laser," *IEEE J. Quantum Electron.*, vol. QE-19, pp. 1391-1397, Sept. 1983.
[21] B. Daino, P. Spano, and S. Piazzolla, "Phase noise and spectral line shape in semiconductor lasers," *IEEE J. Quantum Electron.*, vol. QE-19, pp. 266-270, Mar. 1983.
[22] K. Vahala and A. Yariv, "Semiclassical theory of noise in semiconductor lasers—Part I," *IEEE J. Quantum Electron.*, vol. QE-19, pp. 1096-1101, June 1983.
[23] ——, "Semiconductor theory of noise in semiconductor lasers—Part II," *IEEE J. Quantum Electron.*, vol. QE-19, pp. 1102-1109, June 1983.
[24] K. Vahala, C. Harder, and A. Yariv, "Observation of relaxation resonance effects in the field spectrum of semiconductor lasers," *Appl. Phys. Lett.*, vol. 42, pp. 211-213, Feb. 1983.
[25] W. Elsasser and E. O. Gobel, "Multimode effects in the spectral linewidth of semiconductor lasers," *IEEE J. Quantum Electron.*, vol. QE-21, pp. 687-692, June 1985.

Isabelle Petitbon was born in Paimpol, France, in 1960. She received the Diplôme d'Ingenieur from the Ecole Supérieure de Physique et Chimie and the Diplôme d'Etudes Approfondies in optics and signal processing from the University of Orsay, Orsay, France, in 1984.

Since 1984 she has been with the Ecole Nationale Supérieure des Télécommunications (ENST), Paris, France, where she presently completing work towards the Doctorat de Physique. Her work at ENST has primarily concerned the properties of optically-injected semiconductor lasers and their applications, especially in optical communications.

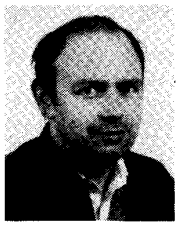

Philippe Gallion (M'83) was born in Saint-Dizier, France, in 1950. He received the Maîtrise de Physique in 1972, the Doctorat de 3° cycle in 1975 from the University of Reims, Reims, France, and the Doctorat d'Etat in 1986 from the University of Montpellier, Montpellier, France.

In 1978 he joined the Ecole Nationale Supérieure des Télécommunications (ENST), Paris, France, where he is presently a Professor of Quantum Electronics and Optical Communications. His research concerns the coherence and modulation properties of semiconductor lasers and coherent optical communication systems.

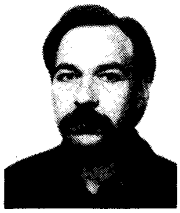

Guy Debarge was born in Clermont-Ferrand, France, on January 31, 1948. He received the Maîtrise de Physique in 1971 and the Doctorat de 3° cycle in 1976 from the University of Clermont-Ferrand.

After conducting research on organic semiconductors at the University of Clermont-Ferrand, he joined the Ecole Nationale Supérieure des Télécommunications (ENST), Paris, France, in 1983. His research has concerned coherent optical communications, coherence properties of semiconductor lasers, and polarization properties of optical fibers.

Claude Chabran was born in Marseille, France, in 1941. He received the master graduation level from the Ecole d'Electricité of Marseille in 1962.

He joined the Ecole Nationale Supérieure des Télécommunications (ENST), Paris, France, in 1984, where he currently heads the Quantum Electronics and Optical Communications Laboratory. He is presently engaged in research on semiconductor laser properties and optical communication systems.